Hyperspectral temperature and salt dependencies of absorption by water and heavy water in the 400–750 nm spectral range

James M. Sullivan, Michael S. Twardowski, J. Ronald V. Zaneveld, Casey M. Moore, Andrew H. Barnard, Percy L. Donaghay, and Bruce Rhoades

The temperature and salt dependencies of absorption by liquid water (H_2O) and heavy water (D_2O) were determined using a hyperspectral absorption and attenuation meter (WET Labs, AC-S). Sodium chloride (NaCl) was used as a proxy for seawater salts. There was no significant temperature (Ψ_T) or salt (Ψ_S) dependency of absorption at wavelengths <550 nm. At wavelengths >550 nm, Ψ_T exhibited peaks at ~604, 662, and 740 nm. A small negative trough in Ψ_S occurred at ~590 nm, followed by a small positive peak ~620 nm, a larger negative trough at ~720 nm, and a strong positive peak at ~755 nm. The salt dependency of absorption by heavy water, Ψ_s^H, exhibited a negative power-law shape with very low Ψ_s^H, at wavelengths >550 nm. Our experiments with NaCl, clean open ocean seawater, and artificial seawater support the hypothesis that salts modify the absorption spectra of seawater by modifying the molecular matrix and vibrations of pure water.   © 2006 Optical Society of America

OCIS codes: 010.7340, 010.4450, 120.6200, 120.4530, 280.0280.

1. Introduction

Understanding how the absorption of light by pure liquid water is affected by variable temperature and salt ions (salinity) is vital to researchers making precise *in situ*, remote, or laboratory optical measurements in natural waters. Correction for these effects is important to numerous scientific disciplines (e.g., limnology, oceanography, satellite remote sensing, and chemistry) and measurement techniques (e.g., spectroscopy and photoacoustics).

The shape and magnitude of the absorption spectrum of pure water is a product of its unique intra-

J. M. Sullivan (jsully@gso.uri.edu) is with the Graduate School of Oceanography, University of Rhode Island, South Ferry Road, Narrangansett, Rhode Island 02882. M. S. Twardowski is with the Department of Research, WET Labs, Incorporated, 164 Dean Knauss Drive, Narrangansett, Rhode Island 02882. J. R. V. Zaneveld, C. M. Moore, and A. H. Barnard are with WET Labs, Incorporated, 620 Applegate Street, Philomath, Oregon 97370. P. L. Donaghay is with the Graduate School of Oceanography, University of Rhode Island, South Ferry Road, Narrangansett, Rhode Island 02882. B. Rhoades is with WET Labs, Incorporated, 620 Applegate Street, Philomath, Oregon 97370.

Received 10 October 2005; revised 23 January 2006; accepted 23 January 2006; posted 3 February 2006 (Doc. ID 65253).

0003-6935/06/215294-16$15.00/0

molecular and intermolecular interactions. More specifically, its absorption spectrum is a direct result of the light absorbed at the frequencies (or wavelengths, λ, as frequency is inversely proportional to wavelength) of the molecular vibrations of chemical bonds and interactions within and between water molecules.[1] The oxygen–hydrogen (O–H) bonds within the water molecule can vibrate in several ways: symmetric stretching, asymmetric stretching, and bending. Each of these vibrations has a unique fundamental frequency and absorptive strength.[1] The fundamental vibrations of the intramolecular symmetric stretch ($v1$) and asymmetric stretch ($v3$) of the O–H bonds of the liquid water molecule occur in the infrared (IR) at frequencies (as wavenumber) of 3277 cm^{-1} ($\lambda = 3050$ nm) and 3490 cm^{-1} ($\lambda = 2870$ nm), respectively.[1] The fundamental vibration of the intramolecular bending ($v2$) of the O–H bonds in liquid water occurs at 1645 cm^{-1} ($\lambda = 6080$ nm).[1] The fundamental vibrations of librations (the restricted rotations of molecules) and intermolecular bend and stretches of liquid water occur at even lower frequencies (higher λ) in the IR than the intramolecular vibrations described above. The absorption spectrum of pure water is extremely complex because in addition to absorption at the fundamental frequencies, each fundamental vibration also has harmonic or overtone modes at

higher frequencies (lower λ) that absorb light at different intensities. Additionally, the fundamental frequencies and harmonics of the different vibrations can have frequencies in close proximity that can interact through coupling and resonance and further affect the spectral absorption shape and intensity.

The strongest peak in the IR absorption spectrum of liquid water occurs at a wavelength of ~3000 nm because this wavelength is centered near the fundamental frequencies of the $v1$ and $v3$ stretch vibrations and the second harmonic of the $v2$ bend vibration. Higher harmonics of the $v1$, $v2$, and $v3$ fundamental vibrations occur in the near-infrared (near-IR) to visible spectral region (750–400 nm) between the fourth and eighth harmonics of the fundamental frequencies.[2,3] However, these higher harmonics have less and less absorption efficiency because as the number of the harmonic mode increases by 2, the absorption efficiency of that vibrational mode decreases by a factor of ~10–20. This produces the characteristic visible absorption spectrum of liquid water with ~100 times more absorption in the red and near-IR wavelengths compared to the shorter blue wavelengths, and with shoulders in the absorption spectrum at spectral locations near the harmonic frequencies.[3]

The shape and magnitude of the absorption spectrum of liquid water is further complicated by changes in temperature and additional ions (e.g., salts such as those found in seawater) within the liquid water molecular matrix.[4–11] These factors can affect the absorptive strength and frequency of the different molecular vibrations (fundamental and harmonics) of water.

This study seeks to quantify the magnitude and hyperspectral shape of both the temperature and salt dependency of absorption by pure liquid water in the visible and near-IR wavelengths (400–750 nm). Further, we seek to describe the nature of both effects and illustrate that sodium chloride (NaCl) and the other salt ions in seawater have no significant inherent absorption in the visible and near-IR wavelengths. While previous studies have examined the hyperspectral nature of the temperature dependent absorption of purified water,[6–8,11] to the best of our knowledge, this is the first study to also examine the salt dependent absorption of both purified salt water and heavy salt water (di-deuterium oxide, D_2O) at high spectral resolution in the visible and near-IR wavelengths. Heavy salt water experiments were carried out to test the inherent absorption of NaCl in the visible and near-IR wavelengths. Heavy water was chosen because it has nearly flat absorption spectra between 500 and 750 nm when compared to the complex absorption spectra of H_2O.[2] Natural and artificial seawaters were also examined for comparison to purified NaCl salt water.

2. Methods

All optical measurements were carried out using the AC-S, an *in situ* absorption–attenuation meter (WET Labs, Incorporated, Philomath, Oregon). The AC-S has two 25 cm path-length flow tubes (one side absorption and the other attenuation) and provides measurement outputs at 80+ wavelengths between 400 and 750 nm (~4 nm steps) by using a collimated light source and a linear variable filter (LVF).[12] Individual filter steps have spectral full width at half-maximum (FWHM) bandwidths ranging between ~14 and 18 nm. The absorption channel has a reflecting tube with a diffuser in front of a large area detector at the end of the tube. The attenuation channel has a nonreflective tube and a collimated detector. The AC-S samples at ~4 Hz (and can oscillate a few percent during sampling) and has a measurement precision of ~0.001 m^{-1} and an accuracy of ~0.003 m^{-1}.[12,13]

A. Temperature Dependency of Absorption by Water (Ψ_T)

A clean, 50 l opaque Nalgene™ polyethylene tank was filled with 18.1 MΩ, 0.2 μm filtered de-ionized ultrapure water from a Barnstead E-pure system (model D4641) with an organic-free™ cartridge system. The feed water into the Barnstead E-pure system was supplied by a reverse osmosis system. After filling, the tank was covered and allowed to degas and come to temperature equilibrium for 24 h in a ~23 °C room. At the beginning of each experiment, the AC-S and a Seabird (Bellevue, Washington) SBE-49 conductivity–temperature–depth (CTD) sensor were submerged in the tank to provide simultaneous and continuous measurements of hyperspectral absorption and attenuation and temperature. Prior to submerging the AC-S and the CTD, the exteriors of the instruments were washed with laboratory detergent, thoroughly soaked and rinsed in de-ionized water, and the AC-S optical windows and flow tubes were cleaned with ethanol and lint-free tissue. Just prior to starting each experimental run, the entire exterior of the 50 l tank was surrounded by crushed ice to gradually lower the temperature of the tank water. The 50 l tank was surrounded by a much larger outer container to contain the ice. When the inner tank water reached ~5 °C, the crushed ice was removed from the outer tank and replaced with hot water to gradually raise the temperature of the inner tank water back to ~23 °C. The cooling and heating cycles took approximately 4–5 h each. The changes in water temperature and hyperspectral absorption and attenuation were continually recorded as the temperature cycled. The AC-S had a 0.2 μm filter (Pall maxicapsule, PN 12112) on its intakes to eliminate bubbles and any contamination particles (e.g., airborne dust) from contributing to the optical measurements. Least-squares regressions of the differential change in absorption dependent on temperature were highly linear [Fig. 1(a)]. As a result, we used the slopes of the linear relationships for each discrete wavelength to determine the Ψ_T of pure water. No significant difference was found in the slope of the relationship when measurements were made during either heating or cooling cycles with either the absorption or attenuation channels of the AC-S. Two different AC-S instruments were used in replicate temperature experiments (four independent channel
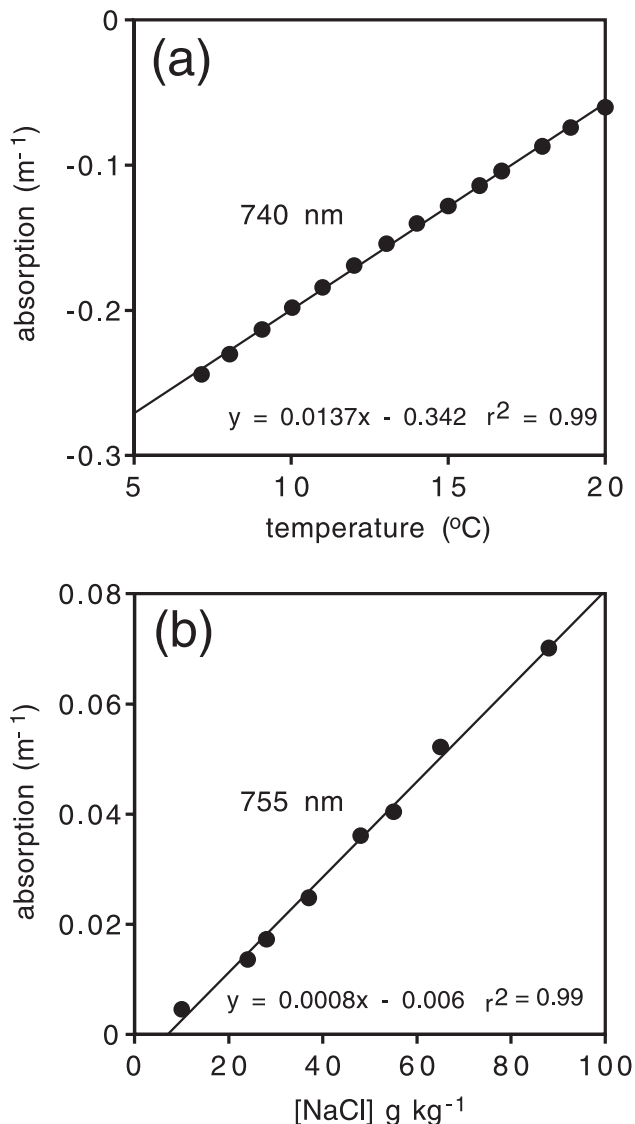
Fig. 1. (a) Least-squares linear regression between temperature (°C) and absorption (m^{-1}) at 740 nm (slope represents Ψ_T). (b) Least-squares linear regression of NaCl concentration and absorption (m^{-1}) at 755 nm (slope represents an approximation of Ψ_S, uncorrected for added molecular scattering from salts). The blank was Barnstead de-ionized water. The most pronounced effects on pure water absorption for temperature and salinity in the visible and NIR are exhibited at these wavelengths, respectively.

measurements). The unique wavelength outputs of the individual AC-S channels were linearly interpolated to normalize the measurement outputs of each channel to identical 2 nm steps so that we could compare results collected by different instruments, as well as examine the effects of changing temperature on absorption and attenuation channels of a single instrument. This step is designed to overcome the fact that the centroid of any given wavelength channel of an AC-S varies between instruments because of slight differences that are inherent in the LVF filters used in the AC-S. This is very different from, for example, a WET Labs AC-9, in which each channel is measured by using a single filter with highly con-

trolled optical characteristics. In addition, this step is required to compensate for the fact that the use of a LVF results in a slight offset of the centroid of wavelengths measured by the absorption and attenuation channels. However, this design has an advantage in that the much closer spacing and linear relationship between adjacent AC-S wavelength channels (compared to the AC-9) allows the use of linear regression analysis to estimate absorption and attenuation values at a common set of wavelengths. In addition, such regression analysis tends to suppress the variability inherent in narrow-channel measurements by taking advantage of the fact that adjacent channels should be highly correlated.

B. Salinity Dependency of Absorption by Water (Ψ_S) and Heavy Water (Ψ_s^H)

All salinity experiments were conducted in a temperature controlled cold room at 15 °C. Before each experimental run the AC-S was allowed to warm up until a stable internal temperature (± 0.1 °C) was reached within the cold room ($\sim$30 min). The absorption of purified fresh water and salt water solutions was measured in the AC-S using the bench-top method described below. All tubing attached to the inflow and outflow ports of the AC-S flow tubes was Tygon™ brand tubing (1/2 in. i.d., PN R-3603) and was wrapped in black tape to eliminate stray light. The tubing was purchased new, cleaned with laboratory detergent, and thoroughly rinsed with de-ionized water. The tubing was never allowed to come into contact with any other solutions but purified fresh water and purified salt water in the experiments, and it was rinsed with 0.2 μm filtered de-ionized water after each experimental run.

A new bench-top AC-S calibration technique was used to minimize the possibility of microbubbles in the sample and to reduce the large sample volume required by the standard continuous-flow calibration method described by Twardowski *et al.*[9] This bench-top setup (Fig. 2) used a single tube that split into a "Y" for the two inflows of each side of the AC-S, with a similar Y joining the two AC-S outflow tubes into a single tube. Prior to the start of each experiment, the AC-S optical windows and flow tubes were cleaned with ethanol and lint-free tissue. The procedure for filling the AC-S with a water sample on the bench top was as follows: the sample was very gently poured into the funnel with the funnel location approximately a foot below the inflow ports of the AC-S. The funnel was slightly tilted to allow the water sample to smoothly flow into the tubing, avoiding any bubble creation through excessive mixing. A small "U" was created by the tubing and funnel below the AC-S inflow (see Fig. 2), and after a small amount of filling, the water sample began to back up into the funnel. At this point, the funnel was slowly raised toward the height of the AC-S inflow tubes while being filled to keep the funnel nearly full. When the funnel position reached just below the height of the AC-S outflow tubes, the AC-S was slowly tilted back at a slight angle ($\sim$30°) to allow any trapped bubbles in the flow

Fig. 2. Illustration of the AC-S bench-top setup used in salinity experiments.

cells to escape, after which the funnel position was gently raised above the outflow tubes. The AC-S was then returned to its normal upright position and continuous measurements on the sample were taken for approximately 3 min.

This bench-top method was used to calibrate the AC-S (analogous to a spectrophotometric blank using purified water) and produced identical, reproducible results to calibrations done using the standard AC-9 calibration protocol developed by Twardowski *et al.*[9] This standard AC-9 method entails continually flowing pressurized purified water through the flow cells. In fact, using the bench-top method described above to calibrate WET Labs AC devices was easier and faster than the standard calibration method, did not require the extra equipment (e.g., a pressurized nitrogen tank, a regulator, and large polycarbonate carboys), and used less purified water. When filled, the entire volume of the Tygon tubing and the two AC-S flow tubes was ~200 ml. Four replicate calibration measurements required less than 1 l of purified water.

Because of the extreme difficulty in removing all optical impurities from natural seawater,[8,9] the primary experiments to determine the salinity depen-

dency of pure water absorption were carried out with 99.9% pure optical grade NaCl (Aldrich Chemical Company, PN 37886-0) dissolved in 18.1 MΩ deionized water produced from the Barnstead E-pure system described in Section 1. The optical grade NaCl salt was assayed by the manufacturer and contained no measurable carbon [chromophoric dissolved organic matter (CDOM) is a potential absorbing contaminant]. The ions Na^+ and Cl^- make up the bulk (~86%) of the ion species in seawater by mass (nine other major ion constituents account for the remaining ~14%), and we hypothesized that solutions of seawater or strictly NaCl with identical mass ion concentrations would have essentially identical effects on pure water absorption. Stated another way, we are assuming that NaCl can act as a good proxy (on a mass basis) for the other ions in seawater in the context of assessing the perturbation of the pure water molecules and resulting absorption effects due to the water molecule and salt ion interactions. This hypothesis was tested in parallel experiments carried out with natural seawater and artificial seawater (see below). A more detailed consideration of the ramifications of approximating seawater with NaCl solutions for evaluating the effect on pure water absorption is provided in Section 4.

After adding NaCl to the purified Barnstead deionized water, all solutions were 0.2 μm filtered (Poretics Corporation, PN 13013) and stored in clean, 500 ml polycarbonate containers. Before each experimental run, samples were filtered again and allowed to degas and come to temperature equilibrium in the cold room for a minimum of 24 h. The absorption and attenuation of samples were then measured in the AC-S using the bench-top method in this section.

The linearity of salt dependent absorption was confirmed using several concentrations of NaCl solution [Fig. 1(b)].[8] At this point we will use the symbol $\hat{\Psi}_s$ to represent the approximation of the Ψ_S of seawater with the NaCl solution. To increase the accuracy in determining $\hat{\Psi}_s$, a relatively high concentration of 100 parts per thousand (‰) or g kg^{-1} NaCl solution was prepared. The accuracy was increased by virtue of a stronger optical signal and by carrying out numerous replicate measurements. To determine $\hat{\Psi}_S$, the measurement values for Barnstead de-ionized water were subtracted from those of the 100 g kg^{-1} NaCl solution and the resulting values were divided by the NaCl concentration in g kg^{-1} (100 in this case). For our purposes, this g kg^{-1} value is expected to be essentially equivalent to conventional salinity determinations with conductivity cells for the following reason. Seawater has a total ion mass concentration of 1.005 g kg^{-1} S^{-1},[14] where S is salinity as defined by the Practical Salinity Scale (PSS) 1978.[15] Note here that salinity as defined by the PSS 1978 is a unitless number; however, to avoid confusion, we will hereafter represent PSS 1978 salinity with the abbreviation S. Following our assumption that solutions of seawater or strictly NaCl with identical ionic mass concentrations would have essentially identical effects on

pure water absorption, the 100 g kg^{-1} NaCl solution would be comparable to a solution of seawater with an S of 99.5 (note, however, that the PSS 1978 salinity was technically intended to be applicable only to seawater solutions with conductivities representative of salinities of 2 to 42). PSS 1978 salinities derived in this way are statistically identical to the g kg^{-1} NaCl mass concentrations used here.

To determine the final $\hat{\Psi}_s$ values, the results of 25 experimental runs with the 100 g kg^{-1} NaCl solution were averaged. Similar to temperature measurements, the unique wavelength outputs of each AC-S channel were linearly interpolated to normalize the measurement outputs of each channel to identical 2 nm steps.

To determine the absorption dependency of heavy salt water, Ψ_s^H, the same bench-top protocol as that described above for the NaCl water solutions was used. Purified heavy salt water solutions were made by dissolving 99.9% pure optical grade NaCl (Aldrich Chemical Company, PN 37886-0) into 99.9% pure heavy water (99.9% D$_2$O, Aldrich Chemical Company, PN 151882) at a NaCl concentration of 100 g kg^{-1}. A separate set of clean tubing in the bench-top setup was used for D$_2$O experiments. The tubing was rinsed with purified water after each experimental run and allowed to completely dry to avoid contaminating the D$_2$O with H$_2$O. To determine the final Ψ_s^H coefficients, the results of ten experimental runs were averaged.

The Ψ_S of both natural and artificial seawater were examined for comparison to the $\hat{\Psi}_s$ of the 100 g kg^{-1} NaCl solution. The concern with these seawater solutions is probable contamination from CDOM. Derived Ψ_S values for the seawater solutions are thus represented as Ψ_{S+CDOM}. North Atlantic sea water (NASW) was collected using a Niskin bottle at a depth of ~200 m at location 39.6 N, 70.6 W (~50 km past the NW Atlantic shelf break). The NASW seawater sample was stored for 3 months in a clean, sealed polycarbonate container and had a measured S of 35.6. The artificial sea water (ASW) comprised commercial grade sea salts (Sigma–Aldrich, PN S9883) dissolved in Barnstead de-ionized water to achieve a measured S of 30. In a previous study,[9] this solution was extensively purified after the addition of the salts to remove CDOM contamination from the commercial salt mixture. Since the previous study, the solution has been stored in a polycarbonate container for ~8 yr. The same bench-top protocol as described above was followed here for the NASW and ASW. The results of ten experimental runs were averaged for each of the seawater samples.

C. Spectral Corrections for Bandwidth Smearing

The nature of the AC-S LVF filter and associated bandwidth for each wavelength step will tend to reduce sharp peaks and fill in sharp troughs due to averaging of the spectra over the bandwidth.[16] This is true of any optical device that uses filters with discrete bandwidths. In the strictest sense, the values measured above thus represent the Ψ_T and Ψ_S values specific to measurements of absorption and attenuation made with this AC-S (see Section 4 for more detail). To correct for the over and under estimations of steeply curved sections of absorption spectra in AC-S measurements due to this spectral smearing, Zaneveld et al.[16] developed a derivative correction method using Gaussian filter factors that can recover actual versus measured spectra. Their correction methods were applied to the Ψ_T and Ψ_S spectra measured here to better estimate the actual temperature and salt dependencies of absorption by pure water and corrected and uncorrected spectra were compared.

D. Estimation of Molecular Scattering by Pure Water and Salt Water

The wavelength (λ) and temperature (T) dependency of scattering by pure water was computed from the Einstein–Smoluchowski (E–S) equation, describing the molecular density fluctuations of water.[6,17] The empirical relationships presented by Buiteveld et al.[6] (updated from the values used by Morel[17] describing the λ and T dependencies of the physical variables used in the E–S equation were used here with the following changes: (1) 1.380 65 10^{-23} J K^{-1} was used as the Boltzmann constant, and (2) after reviewing the data of Lepple and Millero[18] cited by Buiteveld et al.,[6] the scaling factor of 10^{-10} was used for the isothermal compressibility of water instead of 10^{-11} as reported (both changes are assumed clerical errors by Buiteveld et al.[6]). For pure water at 20 °C, we obtain the same scattering values as those reported in Table 1 of Buiteveld et al.[6]

The molecular scattering of salt water was then estimated using the approximation made by Morel[17] that adding salts increases scattering according to the relationship $[1 + 0.3S/37]$. Note that this relationship was obtained experimentally with essentially one sample and is expected to have uncertainties of at least ±5%. For the purposes of estimating molecular scattering, we assumed that the NaCl concentration in g kg^{-1} was equivalent to PSS 1978 salinity, following our previous reasoning. For the attenuation measurements, the changes in absorption due to salinity were isolated by subtracting the difference of the molecular scattering of salt water and pure water (note that the molecular scattering of pure water was incorporated in the AC-S calibration blank). For the reflective tube absorption measurement with the AC-S, scattered light from ~0° to ~41.7° is collected by the detector, so molecular scattering was removed by integrating from 41.7° to 180° for both salt water and pure water and subtracting the difference.

3. Results

The temperature dependency of absorption by pure water, Ψ_T, between 400 and 750 nm exhibited small peaks centered at wavelengths of ~604 and 662 nm, and a large peak at ~740 nm, with no significant effect for wavelengths shorter than ~550 nm

(Table 1, Fig. 3). The peaks in Ψ_T correspond to the locations of shoulders in the absorption spectrum of pure water (Fig. 3). Similar to Ψ_T, $\hat{\Psi}_s$ showed no significant absorption effects below wavelengths of ~550 nm. The spectral shape of $\hat{\Psi}_s$ at wavelengths >550 nm was more complex than the simple Gaussian shaped peaks of Ψ_T (Table 1, Fig. 4). A small negative trough in $\hat{\Psi}_s$ occurred at ~590 nm, followed by a small positive $\hat{\Psi}_s$ peak at ~620 nm, and a larger negative trough at ~720 nm. At wavelengths longer than 735 nm, $\hat{\Psi}_s$ values were positive and continually increased. The Ψ_s^H of heavy salt water exhibited an approximate negative power-law shape with the highest negative values in the blue wavelengths and very low Ψ_s^H at wavelengths longer than 550 nm (Fig. 5). The trough and peak structure so evident in the salt water $\hat{\Psi}_s$ was totally absent in the Ψ_s^H of heavy salt water.

Unlike Ψ_T for pure water, there was a significant difference in $\hat{\Psi}_s$ values between the absorption and attenuation channels of the AC-S for the 100 g kg^{-1} NaCl water and heavy water solutions. Although the spectral shape between the two channels was identical in both solutions, $\hat{\Psi}_s$ values determined using attenuation were consistently lower than the values determined from absorption (Table 1, Figs. 4 and 5).

The $\Psi_{S+\mathrm{CDOM}}$ values of natural and artificial seawater were very similar to those of the 100 g kg^{-1} NaCl water solution. The primary difference between $\hat{\Psi}_s$ and $\Psi_{S+\mathrm{CDOM}}$ from the two seawater solutions was a significant power-law dependent absorption effect in the seawater solutions at wavelengths shorter than ~650 nm, consistent with CDOM contamination [Fig. 6(a)]. The power-law dependency was deconvolved from the $\Psi_{S+\mathrm{CDOM}}$ values by fitting a power-law model to the measured absorption spectra between 400 and 550 nm, subtracting the modeled values from the measured values, and recalculating a Ψ_S value without CDOM, which will now be represented as Ψ_s' [Fig. 6(b)]. After deconvolution, Ψ_s' spectra for the seawater samples closely matched the $\hat{\Psi}_s$ of the NaCl solution, and were in fact statistically identical at wavelengths longer than ~460 nm. This is strong evidence that NaCl is a good proxy for seawater.

The measured Ψ_T and $\hat{\Psi}_s$ spectral values described above were first corrected for spectral smearing using the methods of Zaneveld et al.[16] and then for the molecular scattering of salt [Table 2, Fig. 7(a)]. After correction for the molecular scattering of salt, the small increase in $\hat{\Psi}_s$ values measured in the blue wavelengths [compare Figs. 4 and 7(a)] was effectively removed. An important aside is that the commonly used pure water molecular scattering values from Morel[17] did not fully remove this effect in the blue. Considering that the absence of any Ψ_S effect in the blue region of the visible is expected from theory (see Section 4), these results suggest that the Buiteveld et al.[6] data for the molecular scattering of pure water derived from more updated physical

constants are the most accurate available at this time. Furthermore, the most accurate values for the molecular scattering of pure seawater would thus be these pure water values multiplied by $[1 + 0.3S/37]$ (see Section 2).

The absorption channel $\hat{\Psi}_s$ spectrum corrected for bandwidth smearing is believed to represent our best estimate of the "true" pure water absorption dependency on seawater salts, Ψ_S. Thus specific Ψ_S values tailored for any instrument measuring absorption may be obtained by convolving this spectrum with the unique bandwidth characteristics for that instrument. The corrected attenuation channel $\hat{\Psi}_S$ values here contain a salt water refractive index instrument-specific measurement offset and are not shown (see Section 4). Isobestic points (regions of no dependency, i.e., $\Psi_S = 0$) in the Ψ_S absorption spectrum occurred at ~602, 676, and 735 nm [Fig. 7(a)]. The spectral shape of Ψ_S was found to be very similar to the first derivative of the Ψ_T values [Fig. 7(b)].

4. Discussion

A. Temperature Dependency of Water Absorption
Several previous studies have examined the temperature dependency of absorption by pure water in the visible and near-IR wavelengths.[6–8,11] The spectral values of Ψ_T measured here were similar to those in previous studies, with a large Ψ_T peak at ~740 nm and at two smaller peaks ~604 and 662 nm. Small differences (on the order of a few nanometers) in the reported peaks between studies are most likely related to the different instruments and instrument configurations used to make the measurements (e.g., different bandwidths and steps for each discrete wavelength measurement mode). All studies found little or no temperature dependency in absorption at wavelengths shorter than 550 nm, with the exception of Buiteveld et al.[6] who had a constant elevated baseline Ψ_T at wavelengths shorter than 550 nm. This suggests there was a bias error in their measurements. After correcting for spectral smearing, the spectrum for Ψ_T measured here was most similar to the recent measurements by Langford et al.[11] These authors determined Ψ_T for ultrapure water using a narrow bandwidth (~2 nm) configured bench-top model GBC-UV 918 absorption spectrophotometer. The Ψ_T maximum at 740 nm has a peak value of ~0.015 m^{-1} °C^{-1}. This would produce an absorption difference of 0.3 m^{-1} over a 20 °C change in water temperature. Considering the AC-S measurement precision of ~0.001 m^{-1}, and that naturally occurring absorption by the particulate and dissolved material in many oceanic waters can be an order of magnitude lower than this difference, the temperature effect is substantial. Furthermore, the signal measured at near-IR wavelengths is often used to correct for scattering errors in absorption measurements in the visible with reflective tube absorption devices.[19] It is typically assumed that there is negligible absorption from dissolved and particulate material in this spec-

Table 1. Hyperspectral Temperature Dependences (Ψ_T, m^{-1} °C^{-1}) for the Absorption of Pure Water and Salinity Dependencies ($\hat{\Psi}_s$, m^{-1}S^{-1}) for the Attenuation (Subscript *c*) and Absorption (Subscript *a*) of Pure Water Measured with the AC-S[a]

λ (nm)	Ψ_T (m^{-1} °C^{-1})	$\sigma_{\Psi T}$ (m^{-1} °C^{-1})	$\hat{\Psi}_{s,c}$ (m^{-1} S^{-1})	$\sigma\hat{\Psi}_{s,c}$ (m^{-1} S^{-1})	$\hat{\Psi}_{s,a}$ (m^{-1} S^{-1})	$\sigma\hat{\Psi}_{s,a}$ (m^{-1} S^{-1})
400	0.0001	0.0002	−0.000 01	0.000 04	0.000 03	0.000 03
402	0.0001	0.0001	−0.000 02	0.000 04	0.000 03	0.000 03
404	0.0001	0.0001	−0.000 02	0.000 04	0.000 03	0.000 03
406	0.0001	0.0001	−0.000 02	0.000 04	0.000 04	0.000 03
408	0.0000	0.0001	−0.000 02	0.000 04	0.000 04	0.000 03
410	0.0000	0.0001	−0.000 02	0.000 04	0.000 04	0.000 03
412	0.0000	0.0001	−0.000 02	0.000 04	0.000 04	0.000 03
414	0.0001	0.0001	−0.000 02	0.000 03	0.000 04	0.000 03
416	0.0000	0.0001	−0.000 02	0.000 03	0.000 04	0.000 03
418	0.0000	0.0001	−0.000 03	0.000 03	0.000 04	0.000 03
420	0.0000	0.0001	−0.000 03	0.000 03	0.000 04	0.000 03
422	0.0000	0.0001	−0.000 03	0.000 03	0.000 03	0.000 03
424	0.0000	0.0001	−0.000 03	0.000 03	0.000 03	0.000 03
426	0.0000	0.0001	−0.000 03	0.000 03	0.000 03	0.000 03
428	0.0000	0.0001	−0.000 03	0.000 03	0.000 03	0.000 03
430	0.0000	0.0001	−0.000 03	0.000 03	0.000 03	0.000 03
432	0.0000	0.0001	−0.000 03	0.000 03	0.000 03	0.000 03
434	0.0000	0.0001	−0.000 03	0.000 03	0.000 03	0.000 03
436	0.0000	0.0000	−0.000 03	0.000 03	0.000 03	0.000 03
438	0.0000	0.0000	−0.000 04	0.000 03	0.000 03	0.000 03
440	0.0000	0.0000	−0.000 04	0.000 03	0.000 02	0.000 02
442	0.0000	0.0000	−0.000 04	0.000 03	0.000 02	0.000 02
444	0.0000	0.0001	−0.000 04	0.000 03	0.000 02	0.000 02
446	0.0000	0.0001	−0.000 04	0.000 03	0.000 02	0.000 02
448	0.0000	0.0001	−0.000 04	0.000 03	0.000 02	0.000 02
450	0.0000	0.0000	−0.000 04	0.000 03	0.000 02	0.000 02
452	0.0000	0.0000	−0.000 04	0.000 03	0.000 02	0.000 02
454	0.0000	0.0000	−0.000 04	0.000 03	0.000 02	0.000 02
456	0.0000	0.0000	−0.000 04	0.000 03	0.000 02	0.000 02
458	0.0000	0.0000	−0.000 04	0.000 03	0.000 02	0.000 02
460	0.0000	0.0000	−0.000 04	0.000 03	0.000 02	0.000 02
462	0.0000	0.0000	−0.000 04	0.000 03	0.000 02	0.000 02
464	0.0000	0.0000	−0.000 04	0.000 02	0.000 02	0.000 02
466	0.0000	0.0000	−0.000 04	0.000 02	0.000 02	0.000 02
468	0.0000	0.0000	−0.000 04	0.000 02	0.000 02	0.000 02
470	0.0000	0.0000	−0.000 04	0.000 02	0.000 01	0.000 02
472	0.0000	0.0000	−0.000 04	0.000 02	0.000 01	0.000 02
474	0.0000	0.0000	−0.000 04	0.000 02	0.000 01	0.000 02
476	0.0000	0.0000	−0.000 04	0.000 02	0.000 01	0.000 02
478	0.0000	0.0000	−0.000 04	0.000 02	0.000 01	0.000 02
480	0.0000	0.0000	−0.000 04	0.000 02	0.000 01	0.000 02
482	0.0000	0.0000	−0.000 04	0.000 02	0.000 01	0.000 02
484	0.0000	0.0000	−0.000 04	0.000 02	0.000 01	0.000 02
486	0.0000	0.0000	−0.000 04	0.000 02	0.000 01	0.000 02
488	0.0000	0.0000	−0.000 04	0.000 02	0.000 01	0.000 02
490	0.0000	0.0000	−0.000 04	0.000 02	0.000 01	0.000 02
492	0.0000	0.0000	−0.000 04	0.000 02	0.000 01	0.000 02
494	0.0000	0.0000	−0.000 04	0.000 02	0.000 01	0.000 02
496	0.0000	0.0000	−0.000 04	0.000 02	0.000 01	0.000 02
498	0.0000	0.0000	−0.000 04	0.000 02	0.000 01	0.000 02
500	0.0000	0.0000	−0.000 04	0.000 02	0.000 01	0.000 02
502	0.0000	0.0000	−0.000 04	0.000 02	0.000 01	0.000 02
504	0.0000	0.0000	−0.000 04	0.000 02	0.000 01	0.000 02
506	0.0000	0.0001	−0.000 04	0.000 02	0.000 01	0.000 02
508	0.0001	0.0001	−0.000 04	0.000 02	0.000 01	0.000 01
510	0.0001	0.0001	−0.000 04	0.000 02	0.000 01	0.000 01
512	0.0001	0.0001	−0.000 04	0.000 02	0.000 01	0.000 01
514	0.0001	0.0001	−0.000 04	0.000 02	0.000 01	0.000 01
516	0.0001	0.0001	−0.000 04	0.000 02	0.000 01	0.000 01

(*Continued*)

Table 1. (*Continued*)

λ (nm)	Ψ_T (m^{-1} °C^{-1})	$\sigma_{\Psi T}$ (m^{-1} °C^{-1})	$\hat{\Psi}_{s,c}$ (m^{-1} S^{-1})	$\sigma\hat{\Psi}_{s,c}$ (m^{-1} S^{-1})	$\hat{\Psi}_{s,a}$ (m^{-1} S^{-1})	$\sigma\hat{\Psi}_{s,a}$ (m^{-1} S^{-1})
518	0.0001	0.0001	−0.000 04	0.000 02	0.000 01	0.000 01
520	0.0001	0.0001	−0.000 04	0.000 02	0.000 01	0.000 01
522	0.0001	0.0001	−0.000 04	0.000 02	0.000 01	0.000 01
524	0.0001	0.0001	−0.000 04	0.000 02	0.000 01	0.000 01
526	0.0001	0.0001	−0.000 04	0.000 02	0.000 01	0.000 01
528	0.0000	0.0001	−0.000 04	0.000 02	0.000 01	0.000 01
530	0.0000	0.0001	−0.000 04	0.000 02	0.000 01	0.000 01
532	0.0000	0.0001	−0.000 04	0.000 02	0.000 01	0.000 01
534	0.0000	0.0001	−0.000 04	0.000 02	0.000 01	0.000 01
536	0.0000	0.0001	−0.000 04	0.000 02	0.000 01	0.000 01
538	0.0000	0.0000	−0.000 04	0.000 02	0.000 01	0.000 01
540	0.0000	0.0000	−0.000 04	0.000 02	0.000 01	0.000 01
542	0.0000	0.0000	−0.000 04	0.000 02	0.000 01	0.000 01
544	0.0000	0.0001	−0.000 04	0.000 02	0.000 01	0.000 01
546	0.0000	0.0000	−0.000 04	0.000 02	0.000 01	0.000 01
548	0.0000	0.0000	−0.000 04	0.000 02	0.000 01	0.000 01
550	0.0000	0.0000	−0.000 04	0.000 01	0.000 00	0.000 01
552	0.0000	0.0000	−0.000 04	0.000 01	0.000 00	0.000 01
554	0.0000	0.0000	−0.000 04	0.000 01	0.000 00	0.000 01
556	0.0000	0.0000	−0.000 04	0.000 01	0.000 00	0.000 01
558	0.0000	0.0000	−0.000 04	0.000 01	0.000 00	0.000 01
560	0.0000	0.0000	−0.000 04	0.000 01	0.000 00	0.000 01
562	0.0000	0.0000	−0.000 04	0.000 01	0.000 00	0.000 01
564	0.0000	0.0000	−0.000 04	0.000 01	0.000 00	0.000 01
566	0.0000	0.0000	−0.000 04	0.000 01	0.000 00	0.000 01
568	0.0000	0.0000	−0.000 04	0.000 01	0.000 00	0.000 01
570	0.0000	0.0001	−0.000 04	0.000 01	−0.000 01	0.000 01
572	0.0000	0.0001	−0.000 05	0.000 01	−0.000 01	0.000 01
574	0.0001	0.0001	−0.000 05	0.000 01	−0.000 01	0.000 01
576	0.0001	0.0001	−0.000 05	0.000 01	−0.000 01	0.000 01
578	0.0001	0.0001	−0.000 05	0.000 01	−0.000 01	0.000 01
580	0.0002	0.0001	−0.000 05	0.000 01	−0.000 01	0.000 01
582	0.0003	0.0001	−0.000 05	0.000 01	−0.000 01	0.000 01
584	0.0003	0.0001	−0.000 05	0.000 01	−0.000 01	0.000 01
586	0.0004	0.0001	−0.000 05	0.000 01	−0.000 01	0.000 01
588	0.0005	0.0001	−0.000 05	0.000 01	−0.000 01	0.000 01
590	0.0006	0.0001	−0.000 05	0.000 01	−0.000 01	0.000 01
592	0.0006	0.0001	−0.000 05	0.000 01	−0.000 01	0.000 01
594	0.0007	0.0001	−0.000 05	0.000 01	−0.000 01	0.000 01
596	0.0008	0.0001	−0.000 05	0.000 01	−0.000 01	0.000 01
598	0.0009	0.0001	−0.000 04	0.000 01	−0.000 01	0.000 01
600	0.0010	0.0001	−0.000 03	0.000 01	0.000 00	0.000 01
602	0.0010	0.0001	−0.000 03	0.000 01	0.000 01	0.000 01
604	0.0010	0.0001	−0.000 02	0.000 01	0.000 02	0.000 01
606	0.0010	0.0001	−0.000 01	0.000 01	0.000 03	0.000 01
608	0.0010	0.0001	0.000 00	0.000 01	0.000 03	0.000 01
610	0.0009	0.0001	0.000 01	0.000 01	0.000 04	0.000 01
612	0.0009	0.0001	0.000 01	0.000 01	0.000 05	0.000 01
614	0.0008	0.0001	0.000 02	0.000 01	0.000 05	0.000 01
616	0.0007	0.0001	0.000 02	0.000 01	0.000 06	0.000 01
618	0.0006	0.0001	0.000 02	0.000 01	0.000 06	0.000 01
620	0.0006	0.0001	0.000 02	0.000 01	0.000 06	0.000 01
622	0.0005	0.0001	0.000 02	0.000 01	0.000 06	0.000 01
624	0.0004	0.0001	0.000 02	0.000 01	0.000 06	0.000 01
626	0.0003	0.0001	0.000 02	0.000 01	0.000 06	0.000 01
628	0.0003	0.0001	0.000 02	0.000 01	0.000 06	0.000 01
630	0.0002	0.0001	0.000 02	0.000 01	0.000 05	0.000 01
632	0.0001	0.0001	0.000 02	0.000 01	0.000 05	0.000 01
634	0.0001	0.0001	0.000 01	0.000 01	0.000 05	0.000 01
636	0.0000	0.0001	0.000 01	0.000 01	0.000 05	0.000 01

(*Continued*)

Table 1. (*Continued*)

λ (nm)	Ψ_T (m^{-1} °C^{-1})	$\sigma_{\Psi T}$ (m^{-1} °C^{-1})	$\hat{\Psi}_{s,c}$ (m^{-1} S^{-1})	$\sigma\hat{\Psi}_{s,c}$ (m^{-1} S^{-1})	$\hat{\Psi}_{s,a}$ (m^{-1} S^{-1})	$\sigma\hat{\Psi}_{s,a}$ (m^{-1} S^{-1})
638	0.0000	0.0001	0.000 01	0.000 01	0.000 04	0.000 01
640	0.0000	0.0001	0.000 01	0.000 01	0.000 04	0.000 01
642	0.0000	0.0001	0.000 00	0.000 01	0.000 04	0.000 01
644	0.0000	0.0001	0.000 00	0.000 01	0.000 04	0.000 01
646	0.0000	0.0001	0.000 00	0.000 01	0.000 03	0.000 01
648	0.0000	0.0001	−0.000 01	0.000 01	0.000 03	0.000 01
650	0.0000	0.0001	−0.000 01	0.000 01	0.000 03	0.000 01
652	0.0000	0.0001	−0.000 01	0.000 01	0.000 02	0.000 01
654	0.0001	0.0001	−0.000 01	0.000 01	0.000 02	0.000 01
656	0.0001	0.0001	−0.000 02	0.000 01	0.000 02	0.000 01
658	0.0001	0.0001	−0.000 02	0.000 01	0.000 02	0.000 01
660	0.0002	0.0001	−0.000 02	0.000 01	0.000 02	0.000 01
662	0.0002	0.0001	−0.000 02	0.000 01	0.000 02	0.000 01
664	0.0002	0.0001	−0.000 02	0.000 01	0.000 02	0.000 01
666	0.0001	0.0001	−0.000 02	0.000 01	0.000 02	0.000 01
668	0.0001	0.0001	−0.000 02	0.000 01	0.000 01	0.000 01
670	0.0001	0.0001	−0.000 02	0.000 01	0.000 01	0.000 01
672	0.0000	0.0001	−0.000 02	0.000 01	0.000 01	0.000 01
674	0.0000	0.0001	−0.000 03	0.000 01	0.000 00	0.000 01
676	−0.0001	0.0001	−0.000 04	0.000 01	0.000 00	0.000 01
678	−0.0001	0.0001	−0.000 05	0.000 01	−0.000 01	0.000 01
680	−0.0001	0.0001	−0.000 06	0.000 01	−0.000 02	0.000 01
682	−0.0001	0.0001	−0.000 06	0.000 01	−0.000 03	0.000 01
684	−0.0001	0.0001	−0.000 08	0.000 01	−0.000 04	0.000 01
686	−0.0001	0.0001	−0.000 09	0.000 01	−0.000 06	0.000 01
688	0.0000	0.0001	−0.000 10	0.000 01	−0.000 07	0.000 01
690	0.0000	0.0001	−0.000 11	0.000 01	−0.000 08	0.000 01
692	0.0001	0.0001	−0.000 13	0.000 01	−0.000 09	0.000 01
694	0.0002	0.0001	−0.000 14	0.000 01	−0.000 11	0.000 01
696	0.0003	0.0001	−0.000 16	0.000 01	−0.000 12	0.000 01
698	0.0005	0.0001	−0.000 17	0.000 01	−0.000 14	0.000 01
700	0.0007	0.0002	−0.000 18	0.000 01	−0.000 15	0.000 01
702	0.0009	0.0002	−0.000 19	0.000 01	−0.000 16	0.000 01
704	0.0013	0.0003	−0.000 20	0.000 01	−0.000 17	0.000 01
706	0.0017	0.0003	−0.000 21	0.000 01	−0.000 18	0.000 01
708	0.0021	0.0004	−0.000 22	0.000 01	−0.000 19	0.000 01
710	0.0026	0.0004	−0.000 22	0.000 01	−0.000 20	0.000 01
712	0.0032	0.0004	−0.000 23	0.000 01	−0.000 20	0.000 01
714	0.0038	0.0004	−0.000 23	0.000 01	−0.000 20	0.000 01
716	0.0045	0.0005	−0.000 23	0.000 01	−0.000 21	0.000 01
718	0.0054	0.0005	−0.000 24	0.000 01	−0.000 21	0.000 01
720	0.0063	0.0006	−0.000 24	0.000 01	−0.000 21	0.000 01
722	0.0073	0.0006	−0.000 24	0.000 01	−0.000 21	0.000 01
724	0.0083	0.0007	−0.000 24	0.000 01	−0.000 21	0.000 01
726	0.0094	0.0007	−0.000 22	0.000 01	−0.000 20	0.000 01
728	0.0104	0.0007	−0.000 21	0.000 01	−0.000 17	0.000 01
730	0.0113	0.0006	−0.000 17	0.000 01	−0.000 13	0.000 01
732	0.0121	0.0005	−0.000 12	0.000 01	−0.000 08	0.000 01
734	0.0128	0.0004	−0.000 06	0.000 01	−0.000 01	0.000 01
736	0.0133	0.0003	0.000 02	0.000 01	0.000 07	0.000 01
738	0.0136	0.0003	0.000 12	0.000 01	0.000 16	0.000 01
740	0.0136	0.0004	0.000 22	0.000 02	0.000 26	0.000 01
742	0.0133	0.0005	0.000 31	0.000 02	0.000 37	0.000 01
744	0.0129	0.0006	0.000 41	0.000 02	0.000 46	0.000 02
746	0.0124	0.0007	0.000 49	0.000 03	0.000 54	0.000 02
748	0.0116	0.0008	0.000 56	0.000 03	0.000 61	0.000 02
750	0.0107	0.0009	0.000 62	0.000 03	0.000 67	0.000 03

[a]To normalize different channels of the AC-S for averaging, the original wavelength outputs of the AC-S were linearly interpolated and output at regular 2 nm wavelength steps (λ, nm). Standard deviations ($\sigma_{\Psi T}$ and $\sigma\hat{\Psi}_s$) for each measured value are also given. These measured Ψ_T and $\hat{\Psi}_s$ values represent AC-S instrument-specific correction factors.
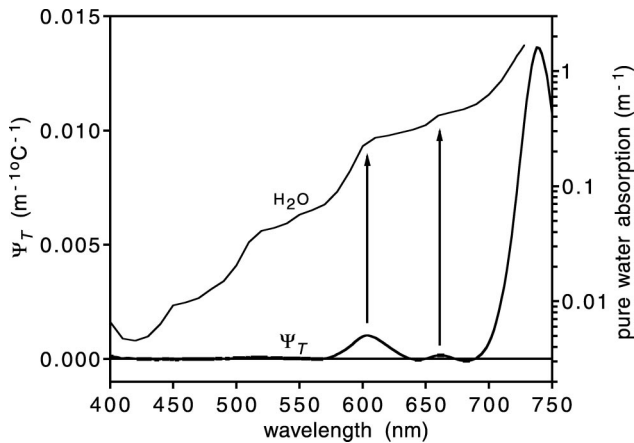
Fig. 3. Temperature dependency of absorption by pure water, Ψ_T (m^{-1} °C^{-1}), using the AC-S (uncorrected for spectral smearing) and the pure water absorption values of Pope and Fry.[3] Arrows indicate the relationship between the locations of Ψ_T and the absorption shoulders of pure water. For estimated uncertainties in Ψ_T see Table 1.

Fig. 5. Salt dependency of absorption by liquid heavy water (D_2O), Ψ_s^H (m^{-1} g^{-1} kg), for the absorption a and attenuation c channels of the AC-S using a NaCl solution. Estimated uncertainties averaged $\sim \pm 0.000\,02$ m^{-1} g^{-1} kg.

tral region and that the signal may be attributed entirely to a scattering error. However, if the measurements have not been accurately corrected for the temperature and salt dependences of pure water absorption, large errors could be introduced.

The spectral shape and location of the Ψ_T peaks of pure water in the visible and near-IR are correlated to the wavelengths of the harmonic combination modes of the fundamental O–H bond vibrational frequencies within liquid water. These characteristic wavelengths also represent shoulders in the absorption spectrum of pure water[3] (see Fig. 3). The anharmonic formula of Tam and Patel[2] predicts the

Fig. 4. Estimates of the salinity dependency of absorption by pure water ($\hat{\Psi}_s$, m^{-1} S^{-1}) for the absorption a and attenuation c channels of the AC-S. Estimates were derived from measurements with a 100 g kg^{-1} NaCl solution. Included are the Ψ_S values of Pegau *et al.*[8] and Twardowski *et al.*,[9] measured using the AC-9 and solutions of artificial seawater. The increase in absorption with decreasing wavelength ≤ 500 nm in this study was found to be attributable to the molecular scattering of salt (see text). For estimated uncertainties see Table 1.
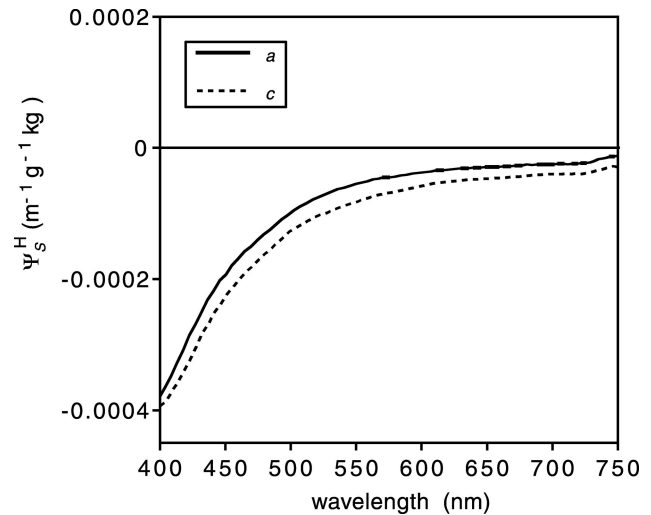
location of the $v1$, $v3$ combination modes as occurring at 742 and 605 nm (fourth and fifth harmonics, respectively), while Pope and Fry[3] added the fundamental of the $v2$ frequency to the $v1$, $v3$ combination mode at 742 nm to predict the 662 nm absorption shoulder. This anharmonic analysis predicts the observed locations of the peak wavelengths for spectral Ψ_T within a few nanometers. Combination modes and frequencies above the fourth and fifth harmonics represent wavelengths shorter than 550 nm, where both the absorption efficiency of the vibrations and thus the pure water absorption coefficient is very low.[3] While some small temperature dependent absorption undoubtedly occurs at wavelengths shorter than 550 nm, measuring its effect at the temperature ranges normally found in fresh water and oceanic environments would most likely require an instrument that could resolve absorption at accuracies near 0.0001 m^{-1} or greater.

B. Salinity Dependency of Water Absorption

While there are a small number of studies that have examined the effects of salts on the absorption of pure water in the IR wavelengths,[10] we are unaware of any published hyperspectral Ψ_S values in the visible and near-IR wavelengths. Pegau *et al.*[8] and Twardowski *et al.*[9] reported Ψ_S values at nine wavelengths between 400 and 750 nm using the WET Labs AC-9, an instrument with similar accuracy and optical geometries for absorption and attenuation as the AC-S. A comparison to our AC-S values (Fig. 4) indicates that their Ψ_S values were slightly higher in the blue wavelengths, probably due to CDOM contamination in their artificial seawater solutions. The purified ASW used by Twardowski *et al.*[9] was also reanalyzed with the AC-S here (compare Figs. 4 and 6), but it showed a more than twofold increase in absorption in the blue region. The previous purification steps (repeated
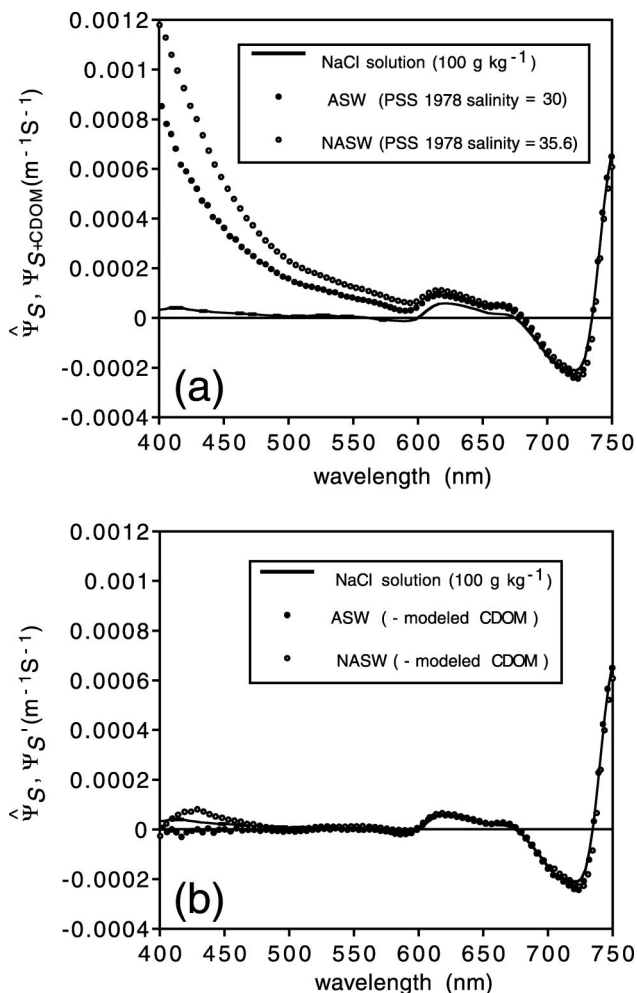
Fig. 6. (a) Salt dependency of absorption for NaCl solution ($\hat{\Psi}_s$, m^{-1} S^{-1}), and NASW and ASW (Ψ_S+CDOM, m^{-1} S^{-1}). (b) Salt dependency of absorption for seawater samples after subtracting CDOM absorption spectra modeled with a power-law relationship (Ψ_s', m^{-1} S^{-1}). The parameter $\hat{\Psi}_s$ is also plotted.

UV photo-oxidation and hydrogen peroxide oxidations) may thus have only temporary effects on CDOM levels.

Pegau *et al.*[8] and Twardowski *et al.*[9] found a significant difference in the values of Ψ_S for the absorption and attenuation channels of the AC-9 ($\sim$0.000 12 and $\sim$0.000 18 m^{-1} S^{-1} difference, respectively). The difference in Ψ_S values (represented as $\hat{\Psi}_s$) between the absorption and attenuation channels of the AC-S averaged $\sim$0.000 04 m^{-1} S^{-1} for the NaCl solution and $\sim$0.000 02 m^{-1} S^{-1} for the heavy water NaCl solution and was spectrally independent. The attenuation channel of the AC-S consists of a fused quartz window, followed by an air gap, and then an optical detector. The absorption channel consists of a fused quartz window with a diffuser and optical detector directly attached (no air gap). Thus light traveling towards the detector in the attenuation side encounters a water–quartz interface and then a quartz–air interface. On the absorption side, the light encounters the water–quartz interface and

then the diffuser. Calculations for the effects of the refractive index of the different solutions and the optical design of the AC-S (e.g., attenuation detector acceptance angle and interface reflectivity) found only the reflectivity effect to be significant. The water–quartz reflectance is a function of the index of the refractions of the two media and thus of salinity. A calculation of the difference in signal between the two channels due to the effect of salinity that takes account of the different reflectivities of the interfaces determined that the attenuation channel of the AC-S should measure $\sim$0.000 02 m^{-1} S^{-1} lower than the absorption channel. Pegau *et al.*[8] also reasoned that the consistently lower Ψ_S values measured in the attenuation channel of the AC-9 were caused by a change in the reflectance at the fused quartz windows due to the increased refractive index of salt water, which these authors calculated would cause the AC-9 attenuation channel to measure $\sim$0.000 05 m^{-1} S^{-1} less Ψ_S than in pure water. Pegau *et al.*[8] further reasoned that without knowledge of the bidirectional reflectance distribution and transmissivity of the absorption channel diffuser, one could not fully correct the absorption channel for this reflectance effect. We theorize that the reflecting tube and large area diffuser in the absorption channel actually reduces or mostly eliminates this effect. This is supported by the observation that the corrected $\hat{\Psi}_s$ values of the AC-S absorption channel are essentially zero in the portions of the visible spectrum (400–550 nm) where the upper harmonic vibrational modes of O–H bonds would predict little or no detectable salt effect. This is analogous to the lack of measurable temperature dependency in the same spectral region. In the 400–550 nm spectral region, the AC-S attenuation channel $\hat{\Psi}_s$ values are negative, and interestingly, by a magnitude very similar to the quartz window reflectance effect value calculated here and by Pegau *et al.*[8]

The presence of salt ions (i.e., Na$^+$ and Cl$^-$) affects the ionic bonding of pure liquid water and produces absorption effects dependent on the salt concentration. The effect of salt ions are varied and can produce absorption band narrowing, frequency vibration shifts, and changes in absorptive intensity of water molecules.[10] Max *et al.*[10] reported that in the IR portion of the water absorption spectrum, disassociated NaCl ions primarily intensified the absorption of the $v1$ molecular vibrations. They suggested that these symmetric stretch vibrations were more sensitive to salt ions than the asymmetric stretch ($v3$) vibrations. Similar differential absorption effects on the molecular vibrations of pure water induced by salt ions also occur in the visible and near-IR. For the Ψ_S spectrum of purified NaCl solutions reported here, we see a dramatic increase in absorption at wavelengths between 735 and 750 nm. Early measurements of a NaCl solution with a prototype AC-S that had spectral range to $\sim$760 nm showed that the Ψ_S peaked at a wavelength $\sim$755 nm.[13] Similar to temperature effects, modification of absorption induced by salt ions

Table 2. Hyperspectral Temperature (Ψ_T, m^{-1} °C^{-1}) and Salinity (Ψ_s, m^{-1} S^{-1}) Dependencies for the Absorption of Pure Water at 2 nm Wavelength Steps (λ, nm)[a]

λ (nm)	Ψ_T (m^{-1} °C^{-1})	Ψ_S (m^{-1} S^{-1})	λ (nm)	Ψ_T (m^{-1} °C^{-1})	Ψ_S (m^{-1} S^{-1})	λ (nm)	Ψ_T (m^{-1} °C^{-1})	Ψ_S (m^{-1} S^{-1})
400	0.0001	0.000 00	518	0.0001	0.000 00	636	0.0000	0.000 04
402	0.0001	0.000 00	520	0.0001	0.000 00	638	0.0000	0.000 04
404	0.0001	0.000 00	522	0.0001	0.000 00	640	−0.0001	0.000 04
406	0.0001	0.000 00	524	0.0001	0.000 00	642	−0.0001	0.000 03
408	0.0000	0.000 01	526	0.0001	0.000 00	644	−0.0001	0.000 03
410	0.0000	0.000 01	528	0.0000	0.000 00	646	−0.0001	0.000 03
412	0.0000	0.000 01	530	0.0000	0.000 00	648	−0.0001	0.000 02
414	0.0001	0.000 01	532	0.0000	0.000 00	650	0.0000	0.000 02
416	0.0001	0.000 01	534	0.0000	0.000 00	652	0.0000	0.000 02
418	0.0000	0.000 01	536	0.0000	0.000 00	654	0.0001	0.000 01
420	0.0000	0.000 01	538	0.0000	0.000 00	656	0.0001	0.000 01
422	0.0000	0.000 00	540	0.0000	0.000 00	658	0.0002	0.000 01
424	0.0000	0.000 00	542	0.0000	−0.000 01	660	0.0002	0.000 01
426	0.0000	0.000 00	544	0.0000	−0.000 01	662	0.0002	0.000 01
428	0.0000	0.000 00	546	0.0000	0.000 00	664	0.0002	0.000 01
430	0.0000	0.000 00	548	0.0000	0.000 00	666	0.0002	0.000 02
432	0.0000	0.000 00	550	0.0000	0.000 00	668	0.0001	0.000 02
434	0.0000	0.000 00	552	0.0000	0.000 00	670	0.0001	0.000 01
436	0.0000	0.000 00	554	0.0000	0.000 00	672	0.0000	0.000 01
438	0.0000	0.000 00	556	0.0000	0.000 00	674	0.0000	0.000 01
440	0.0000	0.000 00	558	0.0000	0.000 00	676	−0.0001	0.000 00
442	0.0000	0.000 00	560	0.0000	−0.000 01	678	−0.0001	−0.000 01
444	0.0000	0.000 00	562	0.0000	−0.000 01	680	−0.0001	−0.000 02
446	0.0000	0.000 00	564	0.0000	−0.000 01	682	−0.0002	−0.000 03
448	0.0000	0.000 00	566	0.0000	−0.000 01	684	−0.0002	−0.000 04
450	0.0000	0.000 00	568	0.0000	−0.000 01	686	−0.0002	−0.000 06
452	0.0000	0.000 00	570	0.0000	−0.000 02	688	−0.0001	−0.000 07
454	0.0000	0.000 00	572	0.0000	−0.000 02	690	−0.0001	−0.000 08
456	0.0000	0.000 00	574	0.0000	−0.000 01	692	−0.0001	−0.000 10
458	0.0000	0.000 00	576	0.0001	−0.000 01	694	0.0000	−0.000 11
460	0.0000	0.000 00	578	0.0001	−0.000 02	696	0.0001	−0.000 13
462	0.0000	0.000 00	580	0.0002	−0.000 02	698	0.0002	−0.000 15
464	0.0000	0.000 00	582	0.0002	−0.000 02	700	0.0004	−0.000 16
466	0.0000	0.000 00	584	0.0003	−0.000 02	702	0.0006	−0.000 17
468	0.0000	0.000 00	586	0.0004	−0.000 02	704	0.0009	−0.000 18
470	0.0000	0.000 00	588	0.0004	−0.000 02	706	0.0012	−0.000 19
472	0.0000	0.000 00	590	0.0005	−0.000 02	708	0.0017	−0.000 20
474	0.0000	0.000 00	592	0.0006	−0.000 02	710	0.0022	−0.000 21
476	0.0000	0.000 00	594	0.0008	−0.000 02	712	0.0027	−0.000 21
478	0.0000	0.000 00	596	0.0009	−0.000 02	714	0.0033	−0.000 21
480	0.0000	−0.000 01	598	0.0010	−0.000 02	716	0.0040	−0.000 22
482	0.0000	−0.000 01	600	0.0011	−0.000 01	718	0.0049	−0.000 23
484	0.0000	−0.000 01	602	0.0011	0.000 00	720	0.0060	−0.000 24
486	0.0000	−0.000 01	604	0.0011	0.000 01	722	0.0071	−0.000 25
488	0.0000	−0.000 01	606	0.0011	0.000 02	724	0.0084	−0.000 25
490	0.0000	−0.000 01	608	0.0011	0.000 03	726	0.0096	−0.000 26
492	0.0000	−0.000 01	610	0.0010	0.000 04	728	0.0108	−0.000 24
494	0.0000	−0.000 01	612	0.0009	0.000 05	730	0.0120	−0.000 21
496	0.0000	−0.000 01	614	0.0008	0.000 05	732	0.0130	−0.000 16
498	0.0000	−0.000 01	616	0.0007	0.000 06	734	0.0139	−0.000 08
500	0.0000	−0.000 01	618	0.0007	0.000 06	736	0.0146	0.000 01
502	0.0000	−0.000 01	620	0.0006	0.000 06	738	0.0150	0.000 12
504	0.0000	−0.000 01	622	0.0005	0.000 06	740	0.0150	0.000 27
506	0.0000	−0.000 01	624	0.0004	0.000 06	742	0.0147	0.000 41
508	0.0001	−0.000 01	626	0.0003	0.000 05	744	0.0142	0.000 54
510	0.0001	−0.000 01	628	0.0002	0.000 05	746	0.0138	0.000 66
512	0.0001	−0.000 01	630	0.0002	0.000 05	748	0.0131	0.000 78
514	0.0001	−0.000 01	632	0.0001	0.000 05	750	0.0124	0.000 89
516	0.0001	0.000 00	634	0.0000	0.000 05			

[a]These values are corrected for spectral smearing and the molecular scattering of salt. These corrected Ψ_T and Ψ_S values are believed to represent our best estimate of the "true" temperature and salt dependencies of pure water. The $\Psi_{S,c}$ corrected values were not used as these values have an instrument-specific offset.
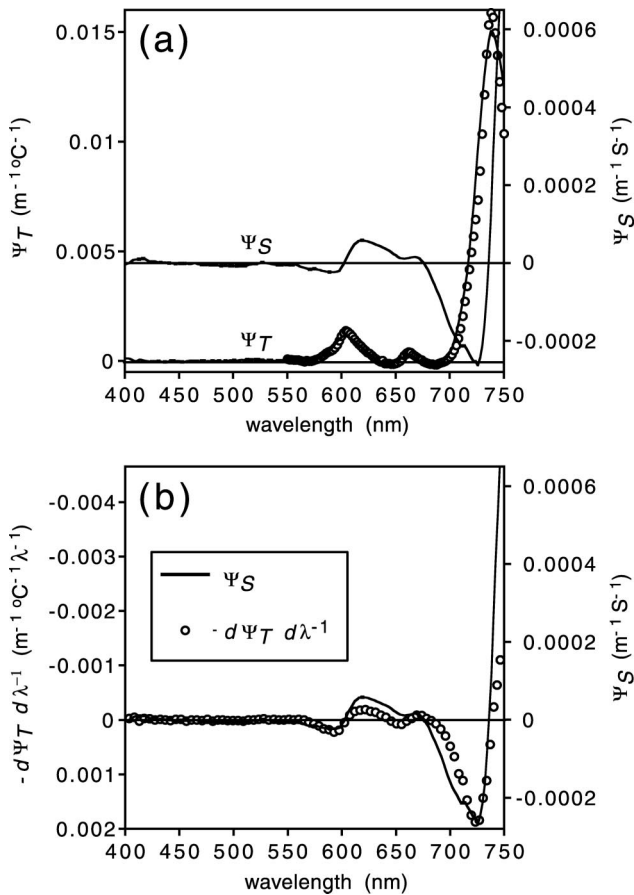
Fig. 7. (a) Final values of the hyperspectral temperature (Ψ_T, $m^{-1}\,°C^{-1}$) and salt (Ψ_S, $m^{-1}\,S^{-1}$) dependency of absorption by pure liquid water after corrections for spectral smearing and the molecular scattering by salts. The open circles represent the Ψ_T values of Langford et al.[11] (b) Comparison of the salt dependency of absorption by pure liquid water (Ψ_S, $m^{-1}\,S^{-1}$) and the first derivative of the temperature dependency of absorption by pure liquid water [$-(d\Psi_T/d\lambda)$, $m^{-1}\,°C^{-1}\,\lambda^{-1}$].

in the visible and near-IR wavelengths occurs near the shoulders of the absorption spectrum of pure water associated with the fourth and fifth harmonic modes of the $v1$, $v3$, and $v2$ vibrations.

It is interesting to note the occurrence of isobestic points in the Ψ_S spectrum near each of the peaks of the Ψ_T spectrum and the similarity of the Ψ_S spectrum to the negative first derivative of Ψ_T, $-(d\Psi_T/d\lambda)$ [Fig. 7(b)]. The spectral peaks in Ψ_T occur near the fourth and fifth harmonic modes of the $v1$, $v3$, and $v2$ fundamental vibrations. For Ψ_T, it appears these vibrations interact through coupling and resonance to enhance the absorptive effect. Conversely, the addition of salt ions into the liquid water molecular matrix appears to affect each of the molecular vibration mechanisms differentially (i.e., one is suppressed while another is intensified), leading to an isobestic point that is in the same location as the peak in Ψ_T. The similarity in spectral shape between Ψ_S and $-(d\Psi_T/d\lambda)$ led to the exciting prospect that perhaps a single model could be developed to explain both the temperature and salinity effects on pure water ab-

sorption. In certain regions longer than 600 nm, however, residuals between the two spectra were significant, and we believe that the temperature and salt effects thus warrant separate treatment. Moreover, while it may be reasonable that the two spectra are similar in shape, the complexity of the interactions between the harmonics of the different vibrations does not lead one to expect the spectra should be identical. This similar shape further supports our hypothesis that salts have no inherent absorption in this spectral region, but rather modify (similar to changes in temperature) the absorption spectra of pure water by modifying the molecular matrix and vibrations of the water. The occurrence of isobestic points also indicates that pure salt water can be thought of as two solutions comprising a mixture of pure water and salt-solvated water.[10]

Our results suggest that common salt (NaCl), the major salt constituent of seawater, has little or no inherent absorption in the 400–750 nm spectral range, but instead interacts with the molecular bonds and organization of the pure liquid water to produce characteristic absorption–vibrational shifts dependent on salt concentration. Further evidence for this conclusion was provided by the examination of the Ψ_s^H of D_2O. In heavy water, D replaces the O–H bonds of H_2O with O–D bonds. The heavier deuterium ions have the effect of significantly decreasing the frequency (i.e., increasing the wavelength) of all of the equivalent O–H vibrational bond locations of H_2O.[20] Thus in liquid D_2O, the equivalent O–D to O–H vibrational modes in the 400–750 nm spectral region are displaced by approximately 1000 nm into the IR, with the effect that D_2O has extremely low absorption (i.e., only weakly absorbing vibrational modes) and a relatively flat absorption spectrum between ~550 and 750 nm as compared to H_2O.[2,20–22] Heavy water does absorb slightly more light than H_2O at wavelengths shorter than 500 nm[2,21,22] and its absorption spectrum continues to increase in an approximate power-law shape into the shorter UV wavelengths.[21,22] Because there are only very weak vibrational-absorption modes between 500 and 750 nm in heavy water, there is little salinity dependency in absorption here. We hypothesize that the inverse (negative) power-law spectral shape of D_2O Ψ_S in the blue wavelengths is due to an absorption shoulder of a larger UV peak that has been shifted or weakened by the presence of salt ions. This hypothesis is analogous to the negative Ψ_S values found in the H_2O Ψ_S spectrum near 720 nm. Max et al.[10] reported similar findings for salt (NaCl) dependency in absorption of liquid water in the IR spectral region. These authors concluded that while NaCl ions produce significant absorption effects through ionic interaction with the pure water molecules and its molecular matrix, the ions themselves have no inherent absorption in the IR spectral range between wavenumbers of ~4800 and 650 cm^{-1} (~2000–15 400 nm). In conclusion, the combined observations of little salt dependency at wavelengths shorter

than 550 nm in purified salt water and at wavelengths longer than 550 nm in purified heavy salt water provide more strong evidence that NaCl has little to no inherent absorption in the 400–750 nm spectral range.

Given the results of experiments comparing the $\hat{\Psi}_s$ of the NaCl solution to that of natural and artificial seawater, we hypothesize that the salt dependency of absorption by pure water is primarily a function of the total mass concentration of the salt ions, i.e., ions in seawater other than Na^+ and Cl^- have similar absorption perturbation effects on Ψ_S on a mass equivalent basis. Natural and artificial seawater salts are composed of ~86% Na^+ and Cl^- ions with the remaining major ion species being Mg^{2+}, Ca^{2+}, K^+, Sr^{2+}, SO_4^{2-}, HCO_3^-, Br^-, $B(OH)_3$, and F^-.[23] The above hypothesis is supported by comparing $\hat{\Psi}_s$ from the NaCl solution to the Ψ_{S+CDOM} of natural and artificial seawater [Fig. 6(a)]. The two spectra are closely matched at the red end of the visible, and the differences between the seawater and NaCl solution spectra in the blue wavelengths were modeled well with a power-law shape consistent with CDOM absorption.[24] After removing this power-law shaped component, the resulting spectra, Ψ_s', closely matched $\hat{\Psi}_s$ [Fig. 6(b)].

It is unlikely that any of the power-law shaped spectral absorption in the blue region of the visible in the seawater samples was caused by seawater components other than the ubiquitously observed CDOM. Independently measured fluorescence excitation-emission matrices (EEMs) verified the presence of humiclike fluorescent DOM in the seawater samples, with broad emission peaks centered at 420 and 440 nm for the NASW and ASW samples, respectively, when excited at 290 nm (data not shown). Additionally, aqueous solutions of other major ionic species in seawater besides Na^+ and Cl^- have been shown to be colorless in the visible.[5] Finally, recent measurements with a capillary waveguide system with a 2 m path length detected no significant absorption in the visible in the dissolved fraction of seawater from the surface of the ultraclear South Pacific Ocean after purified NaCl solution blank corrections were applied.[25] This observation verifies that there is no inorganic substance that can be considered a universal component of seawater that exhibits significant (i.e., measurable at this time) absorption in the visible.

The lack of a salt dependency in pure water absorption between 400 and 550 nm is consistent with theoretical expectations. The harmonic vibrations of pure water are very weakly absorbing in this portion of the spectrum[1,3] and it would seem unlikely that the molecular effects of added salts could produce an absorption magnitude many times greater than the measured inherent absorption of pure water.[3] Additionally, the effect of the temperature dependency of absorption is an order of magnitude greater than that of the salt dependency over the ambient ranges of temperature and salinity found in the ocean ($\sim -2\,°C$–$30\,°C$ in temperature and ~ 0–40 in salin-
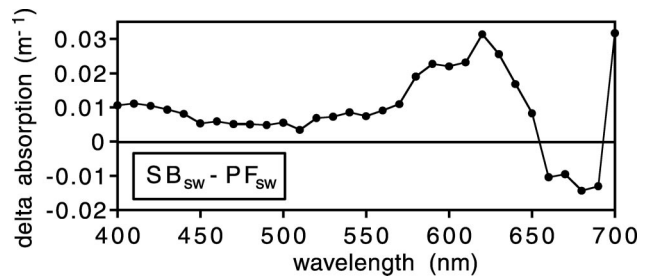

Fig. 8. Difference (delta absorption, m^{-1}) between the clear ocean water values of Smith and Baker[26] (SB_{sw}) and the Pope and Fry[3] pure water values with the addition of the Ψ_S values of this study for salinity of 36 (PF_{sw}).

ity); however, the temperature dependency of the absorption of pure water shows no significant absorption in this region of the visible. In total, these pieces of evidence are all consistent with the conclusion that $\hat{\Psi}_s$, the dependency of pure water absorption on NaCl concentration, is equivalent to Ψ_S, the dependency of pure water absorption on salinity.

The corrected Ψ_S values determined in this study allow the calculation of the hyperspectral absorption spectrum of pure seawater at any salinity by adding the calculated salt absorption values to a known absorption spectrum of pure water (e.g., Pope and Fry[3]). For a theoretical pure seawater at a salinity of 36, the additional absorption induced by salt in the 400–680 nm spectral range is very small, with a maximum magnitude of $\leq 0.002\ m^{-1}$. This is in contrast to the clear ocean water absorption values given in the analysis of Smith and Baker.[26] The residual values for the difference between the values of Smith and Baker[26] and calculated pure seawater absorption (i.e., the Pope and Fry[3] pure water values with salt absorption by a salinity of 36 added) have a fairly consistent offset between 400 and 550 nm; with the values of Smith and Baker[26] being ~ 0.005–$0.01\ m^{-1}$ higher (Fig. 8). The higher values of Smith and Baker[26] may simply represent an instrumental offset or sensitivity (as suggested by Pope and Fry[3]) or an inexact theoretical or experimental assumption carried through their derivations. The residual values in this spectral region do not appear to have the characteristic spectral shape of CDOM contamination as might first be suspected. In the long red and near-IR spectral region (680–750 nm), the additional absorption induced by salt at a salinity of 36 can vary between ~ -0.01 and $0.04\ m^{-1}$. While these are still relatively small values, they are significant and require correction (see discussion in Subsection 4.A for near-IR temperature corrections). At wavelengths longer than 550 nm, the residual values of Smith and Baker[26] have an even higher variable magnitude in comparison to calculated pure seawater. This variation may come from the analysis method used by Smith and Baker,[26] where averaging of different data sets taken at different temperatures and salinities may have occurred.

C. Practical Correction of AC-S Data

The application of the Ψ_T and Ψ_S values for the removal of the temperature and salt dependencies of pure water absorption from AC-S measurements are similar to the methods described for the AC-9.[8,9] Temperature normalization is calculated by

$$a_{\text{tcorr}}(\lambda) = a_{\text{meas}}(\lambda) - (T_i - T_{\text{norm}})^*\Psi_T(\lambda), \qquad (1)$$

where a_{tcorr} is the absorption normalized to a constant temperature, a_{meas} is the absorption measured at the *in situ* temperature, T_i is the *in situ* sample temperature, T_{norm} is the normalization temperature, and $\Psi_T(\lambda)$ is the temperature dependency $(\text{m}^{-1}\,°\text{C}^{-1})$ at the measured wavelength. The relationship is the same for attenuation.

The dependency of salt on absorption is removed by

$$a_{\text{scorr}}(\lambda) = a_{\text{meas}}(\lambda) - S_i^* \hat{\Psi}_{s,a}(\lambda), \qquad (2)$$

$$c_{\text{scorr}}(\lambda) = c_{\text{meas}}(\lambda) - S_i^* \hat{\Psi}_{s,c}(\lambda), \qquad (3)$$

where c_{scorr} is the absorption and a_{scorr} is the attenuation corrected for salt dependency (i.e., normalized to 0 salinity), S_i is the sample salinity, and a_{meas} and c_{meas} are the measured absorption and attenuation coefficients (m^{-1}).

The AC-S Ψ_T and $\hat{\Psi}_s$ measurement values presented here (Table 1) must be used with care when applied to different AC-S instruments. Because of the nature of the AC-S LVF filter, each AC-S has slightly different waveband characteristics (e.g., the FWHM of each wavelength measurement bin, spectral steps, filter transmission, and linear slope characteristics), and applying these coefficients for the removal of all temperature and salinity absorption effects in *in situ* data may leave a residual spectral shape (especially in the strongly sloped near-IR) dependent on the nature of the individual AC-S bandwidth and filter characteristics. Any residual shape after application of these coefficients should be small (e.g., $\sim 0.01\ \text{m}^{-1}$ or less). Specific coefficients could be determined experimentally (as described in this paper) for any specific AC-S to ensure optimal accuracy in applying corrections. This would be desirable for very precise measurements in clear oceanic waters.

Appendix A. List of Symbol Notations

a	Absorption coefficient, m^{-1}
c	Attenuation coefficient, m^{-1}
λ	Wavelength, nm
S	PSS 1978 salinity, unitless
T	Temperature, °C
Ψ_T	Temperature dependency of absorption of pure water, $\text{m}^{-1}\,°\text{C}^{-1}$
Ψ_S	Salt dependency of absorption of pure water using seawater salts, $\text{m}^{-1}\,\text{S}^{-1}$
Ψ_s^H	Salt dependency of absorption of heavy water, $\text{m}^{-1}\,\text{g}^{-1}\,\text{kg NaCl}$
$\hat{\Psi}_s$	Salt dependency of absorption of pure water using NaCl solution, $\text{m}^{-1}\,\text{S}^{-1}$ (see text for explanation of units)
$\Psi_{S+\text{CDOM}}$	Salt dependency of absorption of pure water using natural and artificial seawater with suspected CDOM contamination, $\text{m}^{-1}\,\text{S}^{-1}$
Ψ_s'	Salt dependency of absorption of pure water using natural and artificial seawater with suspected CDOM contamination removed by power-law model, $\text{m}^{-1}\,\text{S}^{-1}$
$v1$	Intramolecular symmetric stretch vibration of liquid water
$v2$	Intramolecular bend vibration of liquid water
$v3$	Intramolecular asymmetric stretch vibration of liquid water
$-(\text{d}\Psi_T/\text{d}\lambda)$	Negative first derivative of Ψ_T

References

1. D. Eisenberg and W. Kauzmann, *The Structure and Properties of Water* (Oxford U. Press, 1969).
2. C. Tam and C. K. N. Patel, "Optical absorption of light and heavy water by laser opto-acoustic spectroscopy," Appl. Opt. **18**, 3348–3358 (1979).
3. R. M. Pope and E. S. Fry, "Absorption spectrum (380–700 nm) of pure water. II. Integrating cavity measurements," Appl. Opt. **36**, 8710–8723 (1997).
4. S. A. Sullivan, "Experimental study of the absorption in distilled water, artificial sea water, and heavy water in the visible region of the spectrum," J. Opt. Soc. Am. **53**, 962–968 (1963).
5. M. Ravisankar, A. T. Reghunath, K. Sathianandan, and V. P. N. Nampoori, "Effect of dissolved NaCl, MgCl$_2$, and Na$_2$SO$_4$ in seawater on the optical attenuation in the region from 430 to 630 nm," Appl. Opt. **27**, 3887–3894 (1988).
6. H. Buiteveld, J. M. H. Hakvoort, and M. Donze, "The optical properties of pure water," in *Ocean Optics XII,* J. S. Jaffe, ed., Proc. SPIE **2258**, 174–183 (1994).
7. I. Trabjerg and N. K. Højerslev, "Temperature influence on light absorption by fresh water and seawater in the visible and near-infrared spectrum," Appl. Opt. **35**, 2653–2658 (1996).
8. W. S. Pegau, D. Grey, and J. R. Zaneveld, "Absorption and attenuation of visible and near-infrared light in water: dependence on temperature and salinity," Appl. Opt. **36**, 6035–6046 (1997).
9. M. S. Twardowski, J. M. Sullivan, P. L. Donaghay, and J. R. V.

Zaneveld, "Microscale quantification of the absorption by dissolved and particulate material in coastal waters with an ac-9," J. Atmos. Ocean. Technol. **16,** 691–707 (1999).

10. J.-J. Max, M. Trudel, and C. Chapados, "Subtraction of the water spectra from the infrared spectrum of saline solutions," Appl. Spectrosc. **52,** 234–239 (1998).

11. V. S. Langford, A. J. McKinley, and T. I. Quickenden, "Temperature dependence of the visible-near-infrared absorption spectrum of liquid water," J. Phys. Chem. A **105,** 8916–8921 (2001).

12. B. Rhoades, A. Derr, C. Moore, and J. R. Zaneveld, "The AC-Spectra, an instrument for hyperspectral characterization of inherent optical properties in natural waters," presented at Ocean Optics XVII, Fremantle, Australia, October 25–29, 2004.

13. J. M. Sullivan, M. S. Twardowski, R. Zaneveld, C. Moore, B. Rhodes, and R. Miller, "The hyper-spectral temperature and salinity dependent absorption coefficients of pure water," presented at Ocean Optics XVII, Fremantle, Australia, October 25–29, 2004.

14. M. E. Q. Pilson, *An Introduction to the Chemistry of the Sea* (Prentice-Hall, 1998).

15. E. L. Lewis, "The Practical Salinity Scale 1978 and its antecedents," IEEE J. Ocean. Eng. **OE-5,** 3–8 (1980).

16. J. R. V. Zaneveld, C. Moore, A. H. Barnard, I. Walsh, M. S. Twardowski, and G. C. Chang, "Correction and analysis of spectral absorption data taken with the WET Labs AC-S," presented at Ocean Optics XVII, Fremantle, Australia, October 25–29, 2004.

17. A. Morel, "Optical properties of pure water and pure seawa-ter," in *Optical Aspects of Oceanography,* N. G. Jerlov and E. Steeman, eds. (Academic, 1974), pp. 1–24.

18. F. K. Lepple and F. J. Millero, "The isothermal compressibility of seawater near one atmosphere," Deep-Sea Res. **18,** 1233–1254 (1971).

19. J. R. V. Zaneveld, J. C. Kitchen, and C. C. Moore, "The Scattering error correction of reflecting tube absorption meters," in *Ocean Optics XII,* S. Ackleson, ed., Proc. SPIE **2258,** 44–55 (1994).

20. C. L. Braun and S. N. Smirnov, "Why is water blue," J. Chem. Educ. **70,** 612–615 (1993).

21. L. P. Boivan, W. F. Davidson, R. S. Storey, D. Sinclair, and E. D. Earle, "Determination of the attenuation coefficients of visible and ultraviolet radiation in heavy water," Appl. Opt. **25,** 877–882 (1986).

22. B. A. Moffat, "The optical calibration of the Sudbury Neutrino Observatory," Ph.D. dissertation (Queen's University, Canada, 2001).

23. F. Culkin, "The major constituents of sea water," in *Chemical Oceanography,* J. P. Riley and G. Skirrow, eds. (Academic, 1965), pp. 121–158.

24. M. S. Twardowski, E. Boss, J. M. Sullivan, and P. L. Donaghay, "Modeling spectral absorption by chromophoric dissolved organic matter (CDOM)," Mar. Chem. **89,** 69–88 (2004).

25. A. Bricaud, Marine Optics and Remote Sensing Laboratory, Laboratoire d'Océanographie de Villefranche, Villefranche-sur-Mer, France (personal communication, 2006).

26. R. C. Smith and K. S. Baker, "Optical properties of the clearest natural waters (200–800 nm)," Appl. Opt. **20,** 177–184 (1981).